Fayoum University Faculty of Engineering, 2024, Vol: 7(2), 106-119
https://fuje.journals.ekb.eg/
ISSN Online: 2537-0634
ISSN Print: 2537-0626

Optimization of Fault Diagnosis of Electrical Motors Using Adaptive Control Based on IOT Monitoring System

Tamer Elkhodragy [1,*], Sayed Osama [1], Mahmoud El Bahy [1]

[1] *Electrical Engineering* Department, Faculty of Engineering, *Benha* University, Benha, Egypt

*Corresponding author: Tamer Elkhodragy (Tamer.Alkhodhary@bhit.bu.edu.eg)

How to cite this paper: Elkhodragy, T., Osam, S. & El Bahy, M. (2024). Optimization of Fault Diagnosis of Electrical Motors Using Adaptive Control Based on IOT Monitoring System. *Journal of Fayoum University Faculty of Engineering, Selected papers from the Third International Conference on Advanced Engineering Technologies for Sustainable Development ICAETSD, held on 21-22 November 2023, 7(2), 106*-119.
https://dx.doi.org/10.21608/fuje.2024.343804

Abstract

Induction motors are popular in industry due to their robustness, reliability, and low maintenance. Like all machines, they can fail and cause downtime, production losses, and safety hazards. Early detection and diagnosis of motor faults prevents catastrophic failures, reduces maintenance costs, and improves efficiency. This paper presents the feasibility and effectiveness of using vibration, temperature, and current (VTC) measurements to obtain a comprehensive picture of the motor's condition and predict faults early. Internet of Things (IoT) sensors and adaptive control supervision protect induction motors by detecting and classifying faults in real-time based on experimental data obtained in the lab. This IoT system monitors and diagnoses electrical motor conditions by measuring VTC to predict functional abnormalities. Sensors are connected to a universal, low-cost microcontroller to obtain the required results. Data is stored on a cloud platform and accessed via a web dashboard and a smartphone application. An efficient adaptive control technique using Artificial Neural Network (ANN) learning identifies fault types even in uncertain diagnosis situations. Simulation results demonstrate its effectiveness in diagnosing the target fault type among the three types. Overall, the paper's results prove that the proposed method improves the reliability and efficiency of motor systems by providing accurate fault diagnosis. This can result in significant economic and environmental benefits by reducing maintenance costs and preventing catastrophic failures.

Keywords

Induction motor, fault prediction, temperature, vibration, current, Internet of Things (IoT), Adaptive control algorithms, Artificial Neural Network, Early detection, Experimental data.

1. Introduction

Industrial processes rely on three-phase induction motors due to their reliability, overload capability, cost-effectiveness, and efficiency. However, faults like unsymmetrical power, unbalanced voltage, and mechanical issues can cause vibration and damage to the stator winding. According to statistical studies of induction motor failure by ASEA Brown Boveri (ABB), the Institution of Electrical and Electronics Engineers (IEEE), and the Electric Power Research Institute (EPRI) shown in Figure 1, bearing and stator defects are the most common types of faults, followed by rotor defects and others [1].

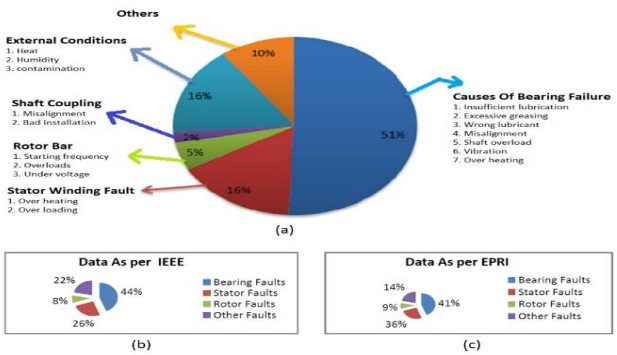

Figure 1. Study on induction motor faults. (a) ABB, (b) IEEE, (c) EPRI

Therefore, identifying and predicting faults before they occur through effective condition monitoring and fault detection is essential to preventing production shutdowns and significant financial losses [2–4]. To ensure safe and reliable operation of industrial induction motors, it's crucial to continuously monitor performance factors, including VTC through VTC sensors, which provide real-time readings, enabling timely repairs and maintenance to prevent motor failures [5–7].

IoT systems have revolutionized induction motor monitoring by enabling real-time monitoring of VTC motor parameters. Cloud-based data storage allows for detailed analysis and detection of potential motor malfunctions. Artificial intelligence (AI) and machine learning enhance data collection processes. ANNs classify motor states as normal or faulty, enabling timely repairs and maintenance to prevent production shutdowns and unexpected failures. Despite challenges in using large mechanical device data for fault prediction, IoT systems offer increased efficiency, reduced energy consumption, and lower operating costs for industrial induction motors [8–10].

This paper begins with a review of the literature, highlighting developments and contributions over earlier investigations. The system design and development are then detailed, including component selection, ideal location, and acquisition methods. The next part discusses the results and comments, as well as MATLAB simulations. Finally, a review of findings and implications concludes the research.

2. Literature Review

Aydil Bapir's research in 2021 focuses solely on bearing faults [11], which are limited to three areas by using different analysis methods: ball, outer race, and inner race. This paper investigates motor faults, including vibration, bearing faults, misaligned loads, improper motor installation, and high temperature of the windings, which can cause insulation damage and failure. Furthermore, we examine motor currents to detect overloading and motor winding problems to monitor and protect the motor from potential damage. ANN is used to assess the condition of the motor and classify faults.

Data collection for Aydil Bapir's study was emailed to the computer as a CSV file and sent to the cloud.

In this paper, data is sent to the cloud and displayed on a web dashboard and mobile application, streamlining ease of use.

In Ekkawach Noyjeen's research in 2021, a temperature sensor is on the motor's external shell, and a vibration sensor measures magnitude without direction [12]. In this paper, for precise winding temperature measurement, the temperature sensor was installed on the motor windings. Furthermore, the vibration sensor was used to read vibration in three axes (x, y, and z) to determine the cause of vibration.

3. System Design and Development

3.1. System Overall

The health monitoring system designed for the electrical motor is in Figure 2. The system is designed to monitor and display the performance of an induction motor produced by Shoubra Co. for Engineering Industries (a Ministry of Military Production company) under a Siemens license.

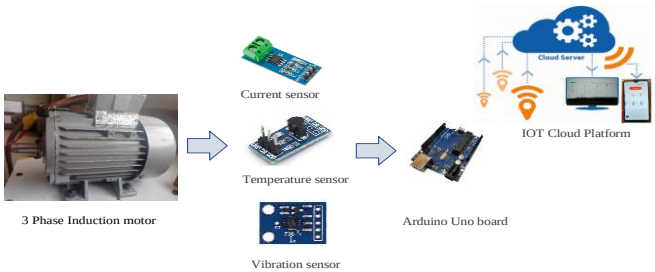

Figure 2. Health monitoring system for the electrical motor

The motor is a three-phase squirrel cage model with a 1 hp rating, 1500 RPM speed, 380Vrms voltage, 50Hz frequency, and 1.95A current. The system utilizes an Arduino Uno R3 microcontroller to operate three single-phase ACS712 current sensors, three digital DS18B20 temperature sensors, and a 3-axis accelerometer ADXL335 vibration sensor.

Laboratory testing ensured the accuracy and validity of motor readings by measuring various factors such as temperatures, current flow, rotational speed, torque, and vibration. Through accurate comparisons with programmed sensor readings, the verified setup ensured proper functioning. For optimum fault detection, the electrical motor securely fastens nuts and bolts, while sensors are carefully positioned for accurate readings, as described below:

3.1.1. Temperature sensor

To ensure precise monitoring of the temperature of each phase winding in a class F motor (which can withstand an ambient temperature of up to 40 °C, a maximum temperature rise of 105 °C, and a maximum allowable temperature of 155 °C) [13], a temperature sensor was securely installed on each winding. To provide accurate temperature measurements, the sensor was chosen based on this insulation categorization [14]. The DS18B20 temperature sensor was chosen for its accuracy, reliability, and ease of use. With a range of -55°C to +125°C and 0.0625°C resolution, it is ideal for motor windings and remote monitoring. The sensor's effectiveness in accurately measuring temperature was confirmed using the Raytek Raynger St2 Infrared Thermometer, which is crucial for optimal and safe motor operation.

It features a user-configurable resolution of 9 to 12 bits, with increments from 0.5°C to 0.0625°C. With its unique one-wire interface, multiple sensors can be connected to a single bus, simplifying monitoring of multiple areas without complicated wiring. Additionally, it is easily interfaced with a microcontroller for real-time monitoring and control, and has low power consumption for continuous monitoring. Its small form-factor and motor winding mounting capability make it an ideal choice for various industrial applications.

In Figure 3. the sensor uses a parasitic power supply, but it can also be powered externally. This option is useful when the sensor is far from the microcontroller. Data pin communicates temperature readings to the microcontroller. Thermistor error curve is shown in Figure 4.

(a)

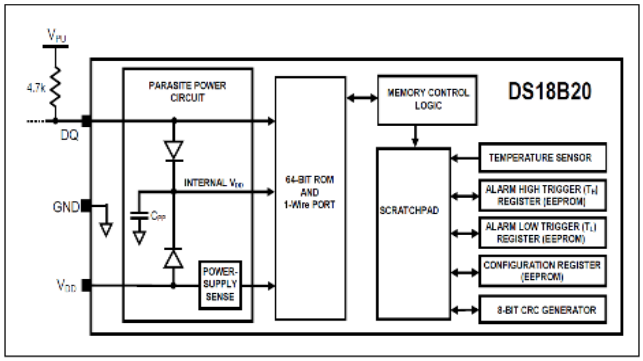

(b)

Figure 3. (a) DS18B20 Sensor chip. (b) Schematic Diagram

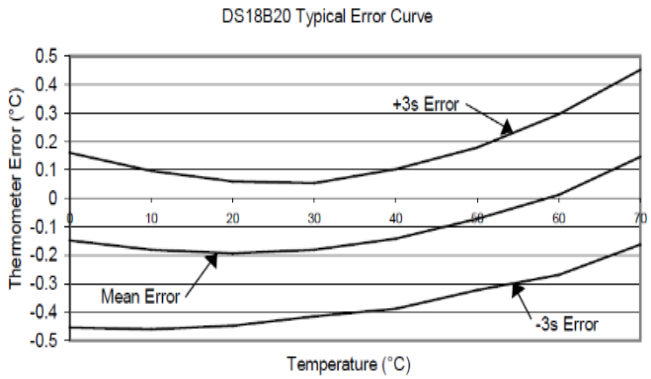

Figure 4. Shows Thermistor's typical error curve that mainly shows these T-sensors have a -0.2◦C bias and a -3 standard deviation error less than 0.3◦C

3.1.2. Current sensor

The current in each phase of the motor was monitored using three current sensors installed on the motor cable. Sensor accuracy was verified using the Fluke 125 multimeter, and the sensors were programmed to ensure precise measurements [15–16]. The ACS712 current sensor's built-in Hall Effect technology, easy installation, ability to measure both AC and DC currents, low noise level, and high isolation between input and output pins make it an accurate and safe option for monitoring the current of a three-phase induction motor.

In Figure 5. the ACS712 uses a Hall Effect integrated circuit (IC) to measure the magnetic field generated by the current flowing through the conductor. which is converted into a voltage proportional to the current, as represented in equation (1).

$$\boldsymbol{V_{out}} = \frac{\boldsymbol{Vcc}}{\boldsymbol{2}} + (\boldsymbol{Sensitivity\ x\ I}) \quad (1)$$

Where; Vcc: Supply voltage, Sensitivity: Sensor sensitivity, I: Conductor current.

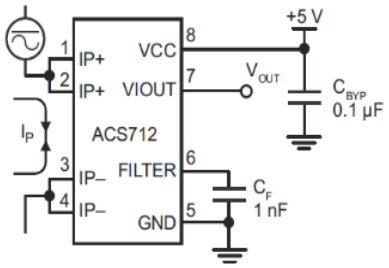

Figure 5. (a) ACS712 sensor chip. (b) ACS712 Internal Schematic Diagram

In Figure 6. the nominal sensitivity and transfer characteristics of the ACS712-05B sensor are shown, which is powered by a 5.0-volt supply. The drift in the output is the minimum for a varying operating temperature.

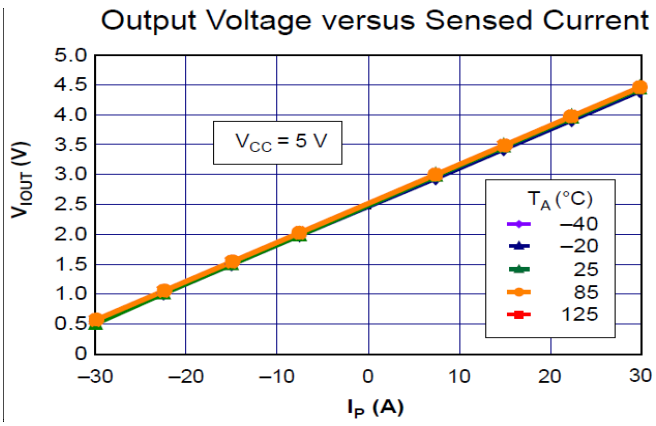

Figure 6. Output voltage vs sensed current of ACS712-05B at 5.0 V power supply and varying temperature

3.1.3. Vibration sensor

For accurate monitoring of motor vibration levels, a vibration sensor was installed at the optimal location on the bearing. It measures vibration in three axes (X, Y, and Z) and can detect the source of vibration, including bearing issues, motor fixing bolts, misalignment, or uneven surfaces [17–19].

The optimal location for vibration sensor installation was determined through an experiment comparing the readings of two sensors: one installed on the bearing and another on the motor junction box.

The analysis of laboratory readings confirms that installing the sensor on the bearing provides more accurate results.

Figure 7. shows the vibration differences in the three axes between sensor 1 installed on the bearing and sensor 2 on the junction box.

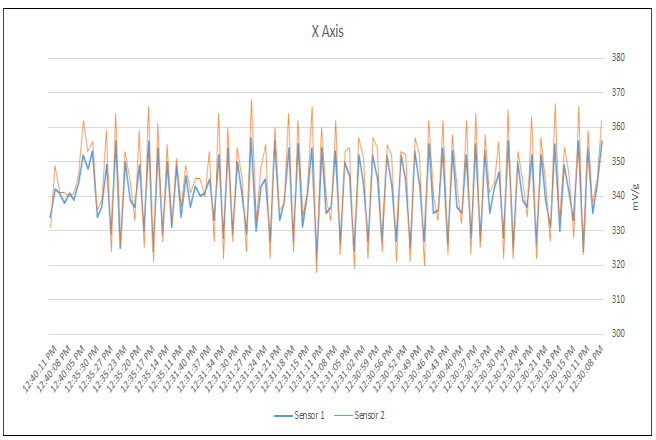

Figure 7. Illustrates the variation in vibrations across the three axes as detected by the two vibration sensors

ADXL335 accelerometer is a highly reliable and low-cost sensor that monitors the vibration of a three-phase induction motor on three axes. It helps plant operators avert unforeseen shutdowns by detecting defects and ensuring regular operation. It measures acceleration in g-forces by sensing changes in capacitance between a fixed plate and a movable proof mass. It functions by measuring acceleration with respect to a fixed frame of reference, as represented by equation (2).

$$Accel_{in\ g} = \frac{Voltage - 1.5\ V}{Sensitivity} \quad (2)$$

Where the sensitivity of ADXL335 is constant at 330 mV/g, giving it a high level of accuracy in measuring accelerations.

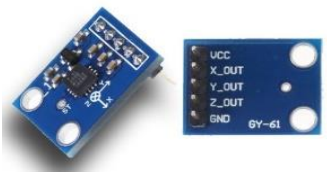

(a)

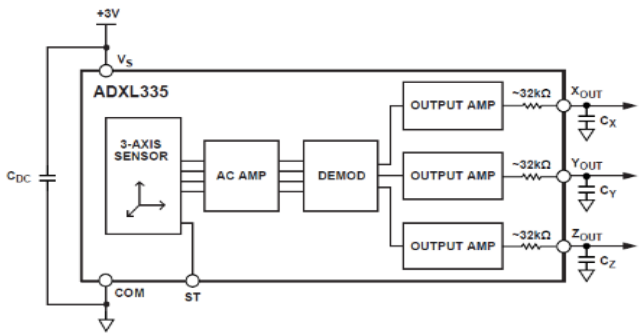

(b)

Figure 8. (a) ADXL335 Accelerometer Sensor. (b) Schematic Diagram

In Figure 8. the ADXL335 sensor has three axes of measurement (X, Y, and Z), with each axis having its own set of components to sense acceleration. The resulting outputs can be read by a microcontroller for real-time monitoring. Moreover, utilizing ANN with ADXL335 enables the analysis of various vibrations, making it possible to distinguish between normal and faulty motors with different fault types having distinct results.

Figure 9. Testing instruments for the electrical motor where (a) Infrared Thermometer (b) Tachometer (c) Digital multimeters (d) Power Analyzer

Figure 9. shows the instruments used for testing the motor.

3.1.4. Microcontroller

The low-cost Arduino Uno microcontroller is ideal for small-scale monitoring projects for 3-phase induction motors and can interface with a variety of sensors and components, making it versatile for multiple monitoring applications [20].

3.2. Data acquisition

Various sensors were meticulously selected to monitor significant parameters for motor performance. Three current sensors provided precise electricity flow measurements of the motor. To analyze thermal performance's impact on efficiency and lifespan, three temperature sensors, one per phase, were mounted on motor windings. Diagnosing mechanical failures due to unbalanced loads or bearing faults relied on a vibration sensor measuring x, y, and z-axis vibration. Collecting data from the sensors for twelve hours daily over a year, under normal and various fault conditions, revealed motor performance. The data analysis identified and categorized transient, short-term, and limit-exceeding readings to accurately identify problems. Laboratory equipment validated sensor accuracy during testing.

Large datasets of up to 20,000 readings of different motor states were utilized for accurate ANN learning used for diagnosing motor faults and determining their actual state.

The project hardware components labeled shown in Fiure10.

3.2.1. Normal and fault conditions Data reading

ANN was trained by conducting laboratory experiments on an electrical motor to collect data on normal and faulty conditions. Deliberate changes were introduced to the motor to simulate different faults, including: a) connecting an unbalanced shaft to create a misalignment load and increase vibration; b) loosening the motor fixing bolts to increase vibration; c) increasing the bearing home of

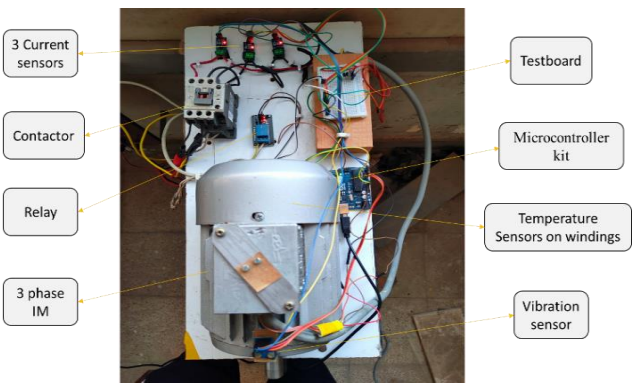

Figure 10. Hardware control of the project

the end shield's diameter by 0.12 mm, which altered the air gap and increased vibration; d) decreasing the bearing home of the end shield's diameter by 0.3 mm, which increased winding temperature and current; e) using a combination of the above methods to create mixed faults. By introducing these faults, a diverse range of data was collected to improve the ANN's ability to detect and diagnose faults in electrical motors.

3.2.2. IoT

An IoT system is developed and connected to a microcontroller kit, enabling easy monitoring of the motor's condition. Motor data is displayed on a web dashboard and a smartphone application, giving users the ability to quickly identify performance ranges and defects. This allows for online motor monitoring from any location at any time.

3.2.3. ANN

An adaptive control technique is employed for accurate diagnosis of the motor's condition using a MATLAB-built ANN.

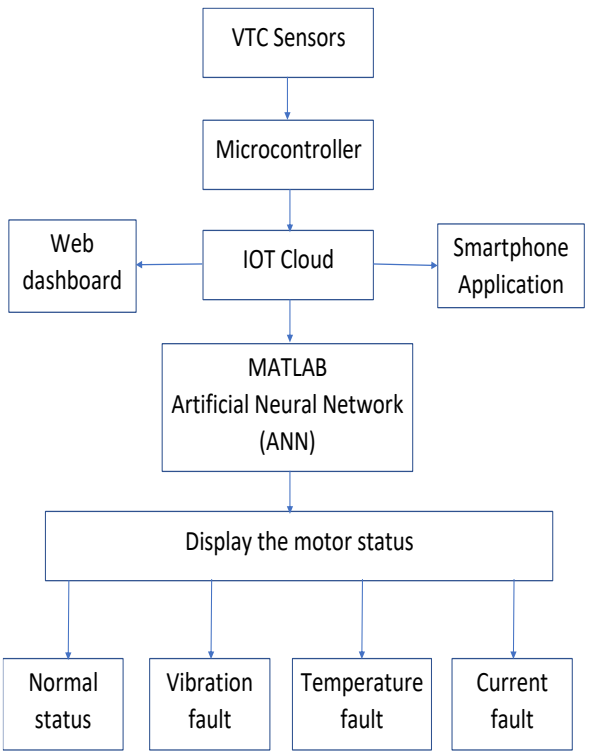

Figure 11. Flowchart model of research context

The ANN is trained on normal and faulty motor data to ensure correct learning and tested to verify the accuracy and validity of its output, which proves to be highly effective.

Then integrated into the project for detecting the motor's actual condition, including healthy condition mode and VTC faults. This improves the diagnosis of motor faults significantly, even in cases of uncertainty.

Figure 11. illustrates the proposed system that installs VTC sensors strategically in optimal locations for accurate data collection. These sensors are connected to a microcontroller kit programmed to read and display data on an Arduino serial monitor, an Excel sheet and the IoT cloud, and then ANN accurately diagnoses the motor's state.

4. Results and Discussion

The circuit was tested in real-time, and the results were categorized into two sections.

4.1. IoT

An operational system was demonstrated that monitored a three-phase induction motor through VTC sensors and an Arduino Uno with WiFi capabilities. The collected data is transmitted to the IoT Blynk cloud and presented in a user-friendly format via a web dashboard and smartphone application, providing real-time data for corrective measures, as shown in Figure 12.

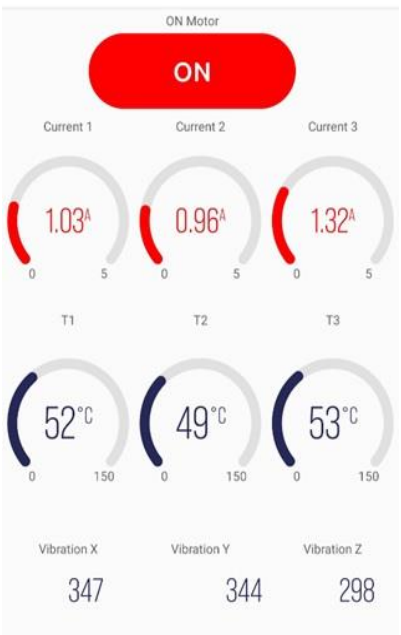

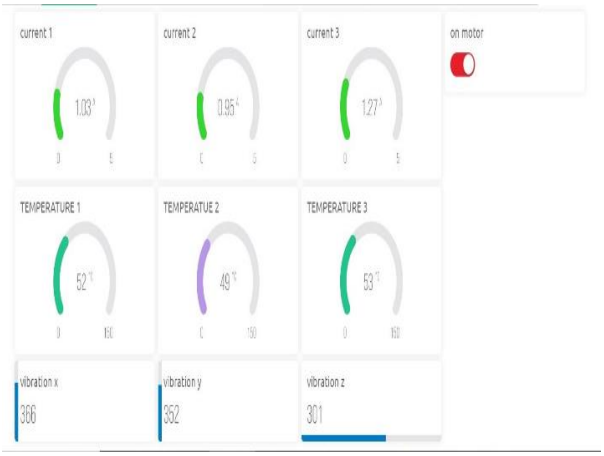

Figure 12. Real image of the IoT smartphone application in first and web dashboard at the bottom which shows a normal-operating motor

4.2. MATLAB

4.2.1. Induction Motor model and Load model

Controlling the speed of an induction motor is critical for numerous industrial applications [21]. The speed of the stator revolving flux (Ns) can be calculated as equation (3):

$$\boldsymbol{Ns = \frac{120f}{p}} \tag{3}$$

Where; f: frequency in Hz, P: number of poles in the machine.

The induction motor per-phase equivalent circuit on the stator side presented in Figure 13.

Where; R1= Stator resistance, X1=Stator leakage reactance, I1=Stator current, Ro=Shunt resistance, Xo=Magnetizing reactance, Io=Per-phase no-load current, V1=Stator voltage, E1 = Stator induced emf.

The machine electrical equation is:

$$Va = IaRa + JXsIa + Eb \tag{4}$$

$$Eb \propto \frac{d\theta}{dt} \tag{5}$$

Electrical torque is: $\boldsymbol{Te = \frac{KE^2 R}{R^2 + X^2}}$ (6)

A. Induction Motor *block diagram and transfer function*

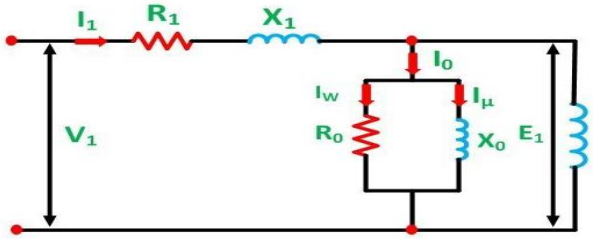

Figure 13. Per-phase equivalent circuit referred to Stator side

Mathematical modeling of an induction motor can be achieved by considering the basic equations of the machine's behavior. From equations (4), (5) and applying La-Place transforms,

$$V_a(s) = I_a(s)(R_a + jX_s) + E_b(s) \tag{7}$$

As is known: $\boldsymbol{E_b = K_t s\theta(s)}$ (8)

Obtained; $V_a(s) = I_a(s)Z(s) + K_t s\theta(s)$ (9)

$$\frac{\boldsymbol{V_a(s) - K_t(s)s\theta(s)}}{\boldsymbol{Z(s)}} = \boldsymbol{I_a(s)} \tag{10}$$

Electrical torque is: $\boldsymbol{T_e = \frac{KE^2 R}{R^2 + X^2}}$ (11)

Taking LaPlace transforms: $\boldsymbol{T_e = E^2 \sin\,\theta}$ (12)

From equation (9) and applying LaPlace transforms:

$$T_m(s) = (Js^2 + Bs)\theta(s) \tag{13}$$

$$\boldsymbol{T_m = T_e \Rightarrow (Js^2 + Bs - E^2)\theta(s) = T_m} \tag{14}$$

$$\frac{\boldsymbol{\theta(s)}}{\boldsymbol{T_m(s)}} = \frac{\boldsymbol{1}}{\boldsymbol{Js^2 + Bs - E^2}} \tag{15}$$

$\boldsymbol{(take\ \theta = 0)}$: $\boldsymbol{T = K\emptyset(s)I_a(s)}$ (16)

$$\frac{\boldsymbol{K_a[V_a(s) - K_t s\theta(s)]}}{\boldsymbol{Z(s)}} = \boldsymbol{(Js^2 + Bs - E^2)\theta(s)} \tag{17}$$

$$\frac{\boldsymbol{\theta(s)}}{\boldsymbol{V_a(s)}} = \frac{\boldsymbol{K_a}}{\boldsymbol{(Js^2 + Bs - E^2)(R_a + L_a s) + K_a K_t s}} \tag{18}$$

Where: $K_a = \frac{3}{2\Pi n_s}$, $K_t = 0.5$, J(Inertia constant) $= 0.076 \text{kgm}^2$, R $= 4.2\Omega$, B(Friction coefficient) $= 8$, L $= 3\text{mH}$.

Transfer function: $G(s) = \frac{\theta(s)}{v_a(s)} = \frac{0.0190}{(1+0.71s)(1+0.0095s)s}$

$$= \frac{0.000128\,S^1+0}{0.00067\,s^3+0.7195\,s^2+s+0} \qquad (19)$$

Using MATLAB Simulink software to generate Figure 14.

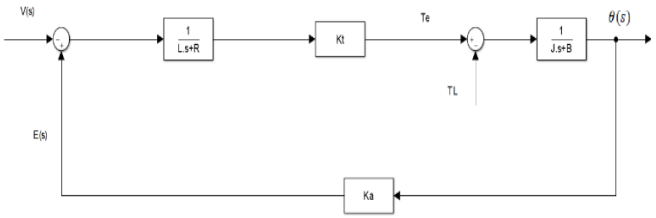

Figure 14. Transfer function block diagram of induction motor

The Load model of induction motor pump shown in figure 15. Where, Va=327<0°, Vb= 327<-120°, Vc= 327<120° at F= 50 HZ.

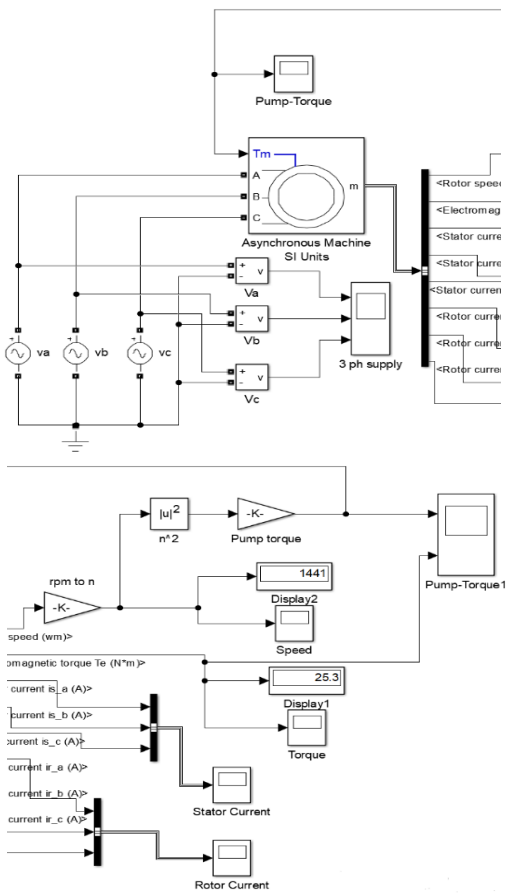

Figure 15. MATLAB Simulink software of three phase induction motor with pump load at running program

plays the unbalanced motor current load and the electromagnetic torque of a 3-phase induction motor given by equations (21) and (22).

In the case of an unbalanced load, Equation (20) dis

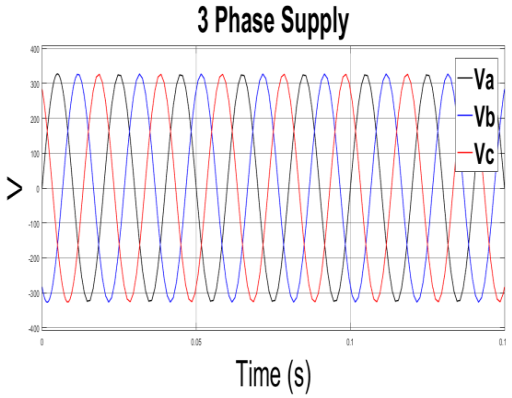

(a)

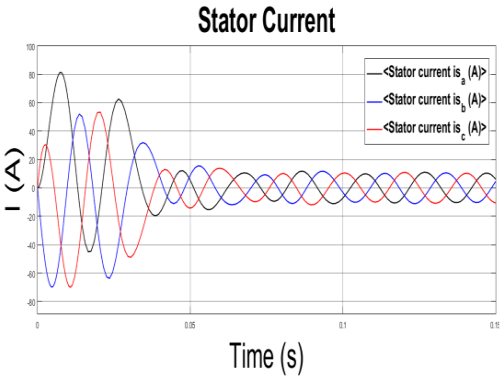

(b)

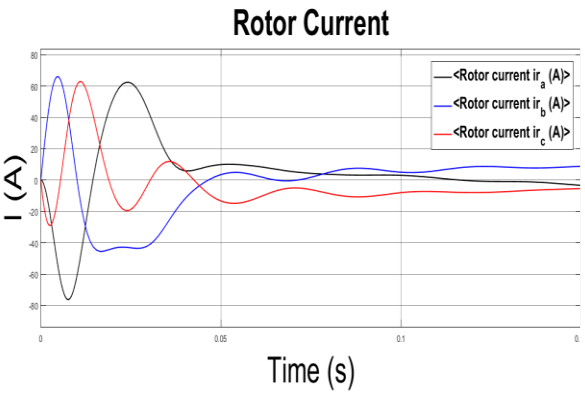

(c)

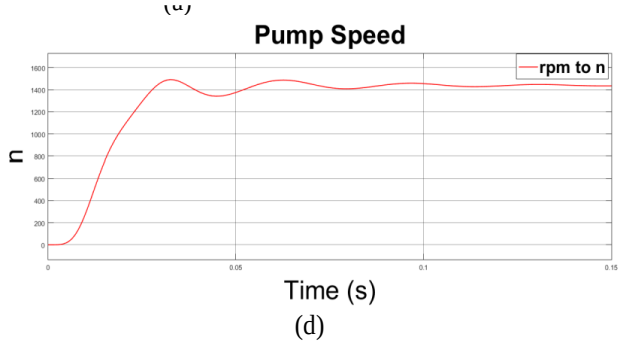

(d)

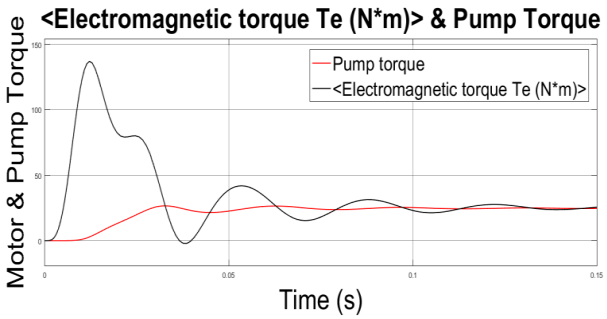

(e)

Figure 16. wave form of (a) the supply voltage matching the pumping-motor (b) Motor stator current I_a, I_b, *and* I_c as function of time (c) Motor rotor current I_a, I_b, *and* I_c as function of time (d) Output response of the pumping-motor speed as function of time

Figure 16. shows MATLAB simulation curves over time of The Load model of induction motor pump.

$$I_{unbal} = (I_1 - I_2) + j(I_3 - I_2) \quad (20)$$

$$\boldsymbol{T_{unbal}} = \left(\frac{3}{2}\right) * \left(\frac{P}{2}\right) * [(\boldsymbol{I_1} - \boldsymbol{I_2}) * \boldsymbol{I_2}\, \boldsymbol{sin}\, \boldsymbol{\theta_2}] \quad (21)$$

$$\boldsymbol{T_{em}} = \left(\frac{3}{2}\right) * \left(\frac{P}{2}\right) * \left(\frac{{I_2}^2}{R_2}\right) * \boldsymbol{S} \quad (22)$$

Where; $\boldsymbol{P}$= number of poles, $\boldsymbol{I_1}, \boldsymbol{I_2}$the stator currents in Phase 1 and 2 respectively, θ2 = angle between the winding of Phase 2 and the rotor axis, $\boldsymbol{R_2}$= stator resistance of Phase 2, $\boldsymbol{S}$ = slip.

4.2.2. ANN model

ANNs are machine learning techniques inspired by the human brain's structure and operation. Comprising interconnected layers of nodes, each with weights and a threshold value. It uses activation functions, such as sigmoid, ReLU, and hyperbolic tangent, to transform inputs from nodes as shown in figure 17. node output in terms of weights, inputs, and activation function in equation (23). It excels in pattern recognition, classification, and prediction tasks, learning complex relationships and making accurate predictions through training and optimization of network weights and thresholds.

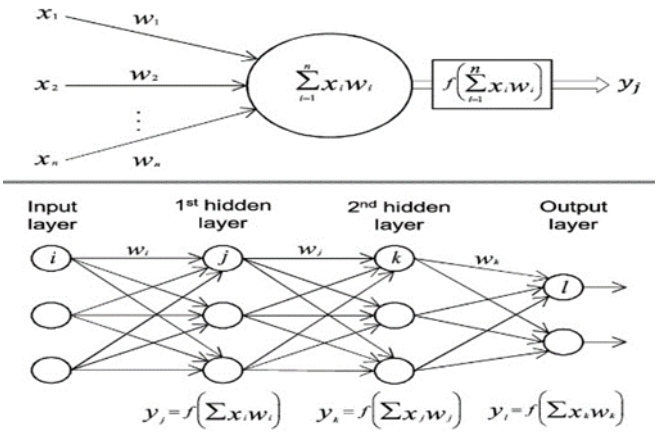

Figure 17. The structure of a Neuron ANN

- Algebraic formula:

$$\sum_{i=1}^{n} \boldsymbol{w_i\, x_i} + \boldsymbol{bias} = \boldsymbol{w_1 x_1} + \boldsymbol{w_2 x_2} + \boldsymbol{w_3 x_3} + \boldsymbol{bias}$$

$$\text{Output} = \boldsymbol{f(x)} = \begin{cases} \mathbf{1}, & \sum \mathbf{w_1 x_1} + \mathbf{b} \geq \mathbf{0} \\ \mathbf{0}, & \sum \mathbf{w_1 x_1} + \mathbf{b} < \mathbf{0} \end{cases} \quad (23)$$

Predicted output =

$$[\boldsymbol{Temperature} \quad \boldsymbol{Vibration} \quad \boldsymbol{Current}][\boldsymbol{Phase}_{(n)}]$$

where n=1,2,3.

$$= [\mathbf{T}_{\emptyset_n} \quad \mathbf{V}_{\emptyset_n} \quad \mathbf{C}_{\emptyset_n}] \quad (24)$$

ANNs exhibit exceptional generalization capabilities, allowing them to detect previously unseen faults.

This means that ANNs can identify faults based on training and measurements, without the need for complex mathematical models [22].

The data from VTC sensors is saved in Excel sheets every three minutes and analyzed using ANN MATLAB software, which analyzes the monitored data.

Figure 18. explains the steps of the ANN program on MATLAB.

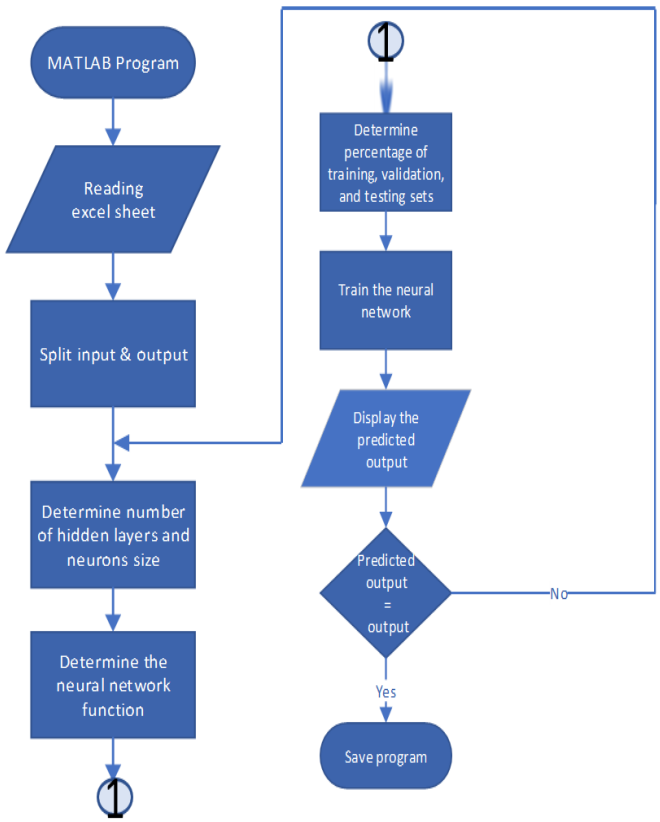

Figure 18. The procedural steps for developing ANN models using MATLAB

Figure 19 shows the structure and algorithms of the model, which uses 2 layers with 10 neurons and TRAINLM training function.

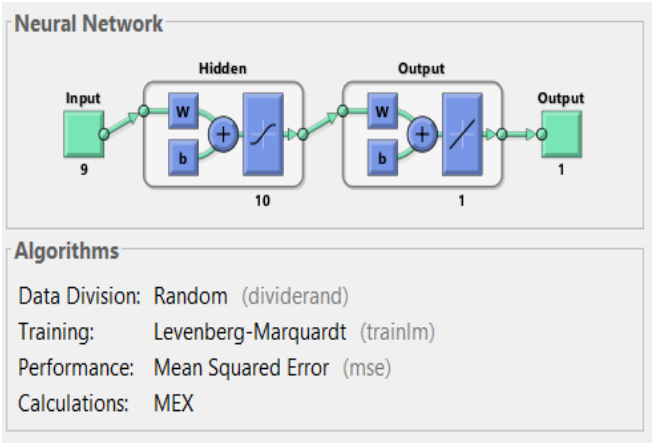

Figure 19. the structure and algorithms of the model

Four ANN motor operation output cases compared in Table I:

Case 1: The normal state (Temperature, vibration and current with range) --- Neural network output = 1.

Case 2: Temperature Fault (Motor winding temperature higher than range) --- Neural network output = -1.

Case 3: Vibration Fault (Motor vibration higher than range) --- Neural network output = -2.

Case 4: Current Fault (Motor phases current higher than range) --- Neural network output = -3.

Table 1

Case	Performance	Training state	Error histogram	Regression
1	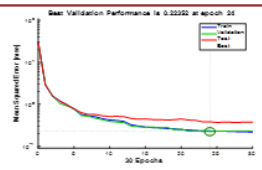	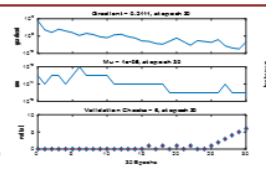	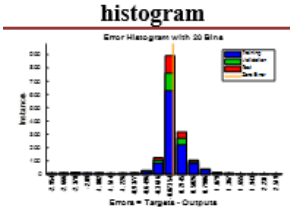	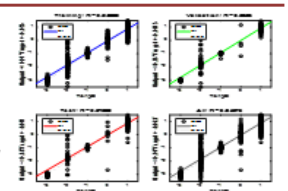
2	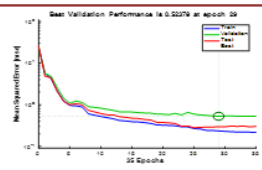	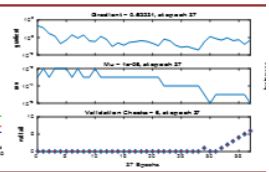	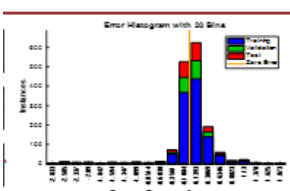	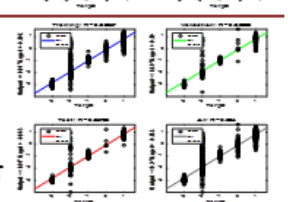
3	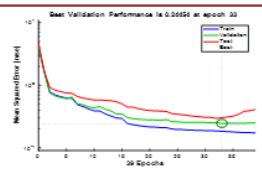	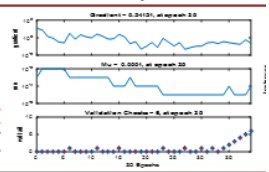	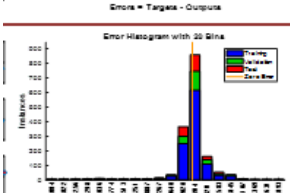	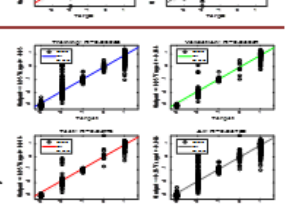
4	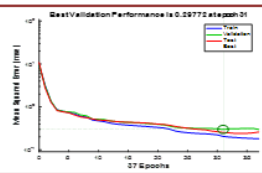	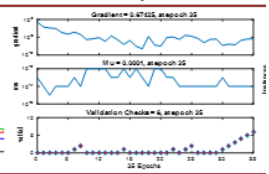	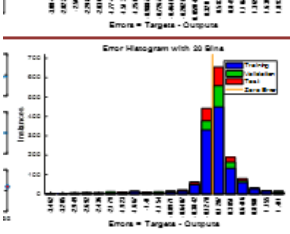	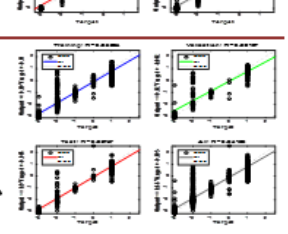

Table 1. Table Of Case Plots Message

Case	Neural network Message

1	Command Window
	New to MATLAB? See resources for Getting Started.
	`>> final_neural_program`
	`The predicted output for new data is: 1`
	`Motor operate in normal condition`
	`fx >>`

2	Command Window
	New to MATLAB? See resources for Getting Started.
	`>> final_neural_program`
	`The predicted output for new data is: -1`
	`Alarm: Temperature Fault`
	`fx >>`

3	Command Window
	New to MATLAB? See resources for Getting Started.
	`>> final_neural_program`
	`The predicted output for new data is: -2`
	`Alarm: Vibration Fault`
	`fx >>`

4	Command Window
	New to MATLAB? See resources for Getting Started.
	`>> final_neural_program`
	`The predicted output for new data is: -3`
	`Alarm: Current Fault`
	`fx >>`

Table 2. Table Of Abbreviations

VTC	Vibration, Temperature, and Current
IoT	Internet of Things
AI	Artificial Intelligence
ANN	Artificial Neural Network
MSE	Mean Squared Error

5. Conclusion

Fault detection is essential for the reliable and efficient operation of industrial induction motors, which necessitates continuous monitoring of various factors, including VTC. Advanced technologies such as IoT systems and ANN can be employed for this purpose.

This paper presents a design system that combines artificial intelligence technology with IoT monitoring systems to facilitate the prediction and diagnosis of electrical motor faults. The system utilizes laboratory testing and sensor strategic placement to ensure accurate motor readings, and stores information in an Arduino program, an Excel sheet, and a cloud platform accessible from multiple locations via an application. A two-layer ANN with 10 neurons and TRAINLM training function achieves high accuracy in predicting motor conditions and classifying VTC faults. The model is trained on a dataset of 10,000 samples, with 70% allocated for training. The achieved accuracy reaches up to 98%, accompanied by a low MSE of $\mathbf{10^{-0.6}}$. Remarkably, the model's running time was only 0.4 milliseconds, facilitating swift and precise predictions. However, when the training function type was modified, the ANN's accuracy decreased to 80%, although with a slightly improved MSE of $\mathbf{10^{-0.42}}$. The modified model's running time increased to 0.6 milliseconds. Continuous monitoring and parameter data analysis enhance motor performance assessment, improving efficiency, accuracy, and system reliability. The Blynk application facilitates remote monitoring, real-time data, and larger-scale monitoring applications.

References

[1] M. Assaeh, "Fault diagnosis of mechanical systems based on electrical supply characteristics." University of Huddersfield, 2019.

[2] A. Jumahat, A. Ahmad, and and M. Z. Abdullah, "Condition-based maintenance of induction motors: A review," J. Mech. Eng. Sci., vol. 11, pp. 4368–4381, 2017.

[3] D. Singh, A. K. Singh, S. K. Singh, and and S. K. Singh, "Condition monitoring of induction motor: A review," Measurement, vol. 157, pp. 107–121, 2020.

[4] Y. Park, H. Choi, J. Shin, J. Park, S. Bin Lee, and H. Jo, "Airgap flux based detection and classification of induction motor rotor and load defects during the starting transient," IEEE Trans. Ind. Electron., vol. 67, no. 12, pp. 10075–10084, 2020, doi: 10.1109/TIE.2019.2962470.

[5] J. Treetrong, "Online failure detection of electric motors," KMUTNB, vol. 22, pp. 436–448, 2012.

[6] N. S. Kumar, B. Vuayalakshmi, R. J. Prarthana, and A. Shankar, "IOT based smart garbage alert system using Arduino UNO," in 2016 IEEE region 10 conference (TENCON), IEEE, 2016, pp. 1028–1034.

[7] M. Iqbal, A. Arshad, and and M. A. Ahmad, "Online condition monitoring of induction motors using vibration and temperature analysis," Autom. Control Eng., vol. 7, pp. 342–348, 2019.

[8] D. Shyamala, D. Swathi, J. L. Prasanna, and A. Ajitha, "IoT platform for condition monitoring of industrial motors," in 2017 2nd International Conference on Communication and Electronics Systems (ICCES), IEEE, 2017, pp. 260–265.

[9] S. B. Kulkarni, V. R. Kulkarni, and and P. S. Moharil, "Fault diagnosis of induction motor using IoT with ANN," Procedia Manuf., vol. 20, pp. 473–478, 2018.

[10] M. S. Al Rawashdeh, B. Al-Khateeb, and and A. Abu-Samaha, "A review of fault diagnosis techniques for induction motors using artificial neural networks," Energies, vol. 13, p. 5662, 2020.

[11] A. BAPİR and İ. AYDIN, "Cloud based bearing fault diagnosis of induction motors," Comput. Sci., no. October, 2021, doi: 10.53070/bbd.990814.

[12] E. Noyjeen, C. Tanita, N. Panthasarn, P. Chansri, and J. Pukkham, "Monitoring Parameters of Three-Phase Induction Motor Using IoT," Proceeding 2021 9th Int. Electr. Eng. Congr. iEECON 2021, pp. 483–486, 2021, doi: 10.1109/iEECON51072.2021.9440368.

[13] Z. Chu, Y. Zhan, and and X. Wang, "Fault diagnosis of class F motor based on multi-point temperature monitoring," IEEE Trans. Ind. Electron., vol. 67, pp. 7742–7751, 2020.

[14] Q. Zhang, Y. Li, and and Y. Zhang, "Real-time temperature monitoring and control of high-power motor windings based on wireless sensor network," IEEE Trans. Ind. Informatics, vol. 15, pp. 489–499, 2019.

[15] M. R. Vinothkanna, "Design and analysis of motor control system for wireless automation," J. Electron. Informatics, vol. 2, no. 3, pp. 162–167, 2020.

[16] N. Bhole and S. Ghodke, "Motor Current Signature Analysis for Fault Detection of Induction Machine–A Review," in 2021 4th Biennial International Conference

on Nascent Technologies in Engineering (ICNTE), IEEE, 2021, pp. 1–6.

[17] "vibration @ www.fluke.com." [Online]. Available: https://www.fluke.com/en-us/products/condition-monitoring/vibration

[18] Q.-H. Zhang, Q. Hu, G. Sun, X. Si, and A. Qin, "Concurrent fault diagnosis for rotating machinery based on vibration sensors," Int. J. Distrib. Sens. Networks, vol. 9, no. 4, p. 472675, 2013.

[19] J. Antoni, "The spectral kurtosis: a useful tool for characterising non-stationary signals," Mech. Syst. Signal Process., vol. 20, no. 2, pp. 282–307, 2006.

[20] A. Choudhary, S. Jamwal, D. Goyal, R. K. Dang, and S. Sehgal, "Condition monitoring of induction motor using internet of things (IoT)," in Recent Advances in Mechanical Engineering: Select Proceedings of NCAME 2019, Springer, 2020, pp. 353–365.

[21] S. Naveen and N. P. Kumar, "Modelling of Induction Motor and Its Performance With Pi,Pid(Nz Method),Pi(Zp) , Fuzzy and Generalised Predictive Control," Int. Res. J. Eng. Technol., pp. 1482–1487, 2016, [Online]. Available: www.irjet.net

[22] G. H. Bazan, P. R. Scalassara, W. Endo, A. Goedtel, W. F. Godoy, and R. H. C. Palácios, "Stator fault analysis of three-phase induction motors using information measures and artificial neural networks," Electr. Power Syst. Res., vol. 143, pp. 347–356, 2017, doi: 10.1016/j.epsr.2016.09.031.